Designing Molecules for Metal−Metal Electronic Communication: Synthesis and Molecular Structure of the Couple of Heterobimetallic Isomers [η^6-(2-Ferrocenyl)indene]-$Cr(CO)_3$ and [η^6-(3-Ferrocenyl)indene]-$Cr(CO)_3$

Saverio Santi,* Alberto Ceccon,* Annalisa Bisello, Christian Durante, Paolo Ganis, and Laura Orian

Dipartimento di Scienze Chimiche, Università degli Studi di Padova, Via Marzolo 1, 35131 Padova, Italy

Franco Benetollo and Laura Crociani

CNR, Istituto di Chimica Inorganica e delle Superfici, C.so Stati Uniti 4, 35127 Padova, Italy

Received April 19, 2005

*Summary: The heterobinuclear isomers [η^6-(2-ferrocenyl)indene]-$Cr(CO)_3$ (**1**) and [η^6-(3-ferrocenyl)indene-$Cr(CO)_3$ (**2**) have been prepared and the crystal structure determination showed that the $Fe(C_5H_5)$ and $Cr(CO)_3$ groups in the two molecules are disposed in different conformations with respect to the Cp-indene bridging ligand, cisoid in **1** and transoid in **2**. Preliminary electrochemical (CV) and spectroscopic (IR and near-IR) results obtained for the corresponding monooxidized $\mathbf{1}^+$ and $\mathbf{2}^+$ demonstrate the existence of stronger electronic coupling in $\mathbf{1}^+$ than in $\mathbf{2}^+$.*

Introduction

Great attention is currently being paid to the study of electronic communication[1] in bimetallic complexes leading to chemical reactions[2] that are unique to the bimetallic species or that are enhanced relative to monometallic compounds. Further, having two metals in close proximity may set up unique physical properties such as luminescence, fluorescence, nonlinear optical activity, redox properties, and charge or energy transfer.[3]

The coordination of two metal nuclei to adjacent sites of rigid or semirigid spacers offers the advantage of finely tuning the factors that rule the intramolecular electronic communication, i.e., the metal−metal distance, the extent of conjugation in the bridging ligand, and the nature of the ancillary ligands. In particular, binuclear complexes having two different metal units are systems of intrinsic interest, as they offer the unique opportunity to explore the dependence of electronic cooperativity on redox asymmetry and of chemical reactivity upon the presence of a second, different redox center in the same molecule. Moreover, the availability of couples of isomers with known geometries should allow the detailed investigation of the effects of slight geometric and electronic modifications of the bridging ligand on the chemical and electronic interaction between the metals. Unfortunately, within the very large set of known homo- and heterobimetallic complexes, only a few examples of pairs of isomers have been characterized and investigated to afford information on the electronic interaction between the metals.[4]

In this work we report the synthesis and characterization of a pair of strictly correlated heterobimetallic isomers, [η^6-(2-ferrocenyl)indene]-$Cr(CO)_3$ (**1**) and [η^6-(3-ferrocenyl)indene]-$Cr(CO)_3$ (**2**) (Scheme 1), whose monooxidized derivatives $\mathbf{1}^+$ and $\mathbf{2}^+$, achievable by chemical or electrochemical oxidation, have been prepared and their electrochemical (CV) and optical (IR and near-IR) properties preliminarily examined.

Scheme 1

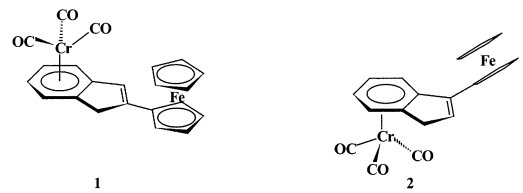

1 2

Results and Discussion

Synthesis and Crystal Structure. The complexes **1** and **2** were prepared by reacting 2- and 3-ferrocenylindene[5] with $(CH_3CN)_3Cr(CO)_3$ in THF (see Supporting Information).

* To whom correspondence should be addressed. E-mail: saverio.santi@unipd.it.

(1) Ceccon, A.; Santi, S.; Orian, L.; Bisello, A. *Coord. Chem. Rev.* **2004**, *248*, 683.

(2) (a) Delville, M.-H. *Inorg. Chim. Acta* **1999**, *291*, 1. (b) de-Azevedo, C. G.; Vollhardt, K. P. C. *Synlett* **2002**, 1019. (c) Santi, S.; Benetollo, F.; Ceccon, A.; Crociani, L.; Gambaro, A.; Ganis, P.; Tiso, M.; Venzo, A. *Organometallics* **2002**, *21*, 565. (d) Degrand, C.; Radecki-Sudre, A. *J. Organomet. Chem*. **1984**, *268*, 63. (e) Yeung, L. K.; Kim, J. E.; Chung, D. Y. K.; Rieger, P. H.; Sweigart, A. *Organometallics* **1996**, *15*, 3891. (f) Bonifaci, C.; Carta, G.; Ceccon, A.; Gambaro, A.; Santi, S.; Venzo, A. *Organometallics* **1996**, *15*, 1630 (g) Burgos, F.; Chavez, I.; Manriquez, J. M.; Valderrama, M.; Lago, E.; Molins, E.; Delpech, F.; Castel, A.; Riviere, P. *Organometallics* **2001**, *20*, 1287.

(3) (a) Barlow, S.; O'Hare, D. *Chem. Rev.* **1997**, *97*, 637. (b) Ward, M. D. *Acc. Chem. Res.* **1998**, *31*, 842. (c) Paul, F.; Lapinte, C. *Coord. Chem. Rev.* **1998**, *178−180*, 431. (d) Belser, P.; Bernhard, S.; Blum, C.; Beyeler, A.; De Cola, L.; Balzani, V. *Coord. Chem. Rev.* **1999**, *190−192*, 155. (e) Heck, J.; Dabek, S.; Meyer-Fredrichsen, T.; Wong, H. *Coord. Chem. Rev.* **1999**, *190−192*, 1217. (f) Benniston, C. A.; Harriman, A.; Li, P.; Sams, C. A.; Ward, M. D. *J. Am. Chem. Soc.* **2004**, *125*, 13630. (g) Roué, S.; Lapinte, C.; Bataille, T. *Organometallics* **2004**, *23*, 2558.

(4) (a) Manriquez, J. M.; Ward, M. D.; Reiff, W. M.; Calabrese, J. C.; Jones, N. L.; Carroll, P. J.; Bunel, E. E.; Miller, J. S. *J. Am. Chem. Soc.* **1995**, *117*, 6182. (b) Liu, T.-Y, Chen, J. Y.; Tai, C.-C.; Kwan, K. S. *Inorg. Chem*. **1999**, *38*, 674. (c) Santi, S.; Ceccon, A.; Carli, F.; Crociani, L.; Bisello, A.; Tiso, M.; Venzo, A. *Organometallics* **2002**, *21*, 2679. (d) Scott, W. E.; Craig, D. C.; Colbran, S. B. *J. Chem. Soc., Dalton Trans.* **2002**, 2423. (e) Cotton, F. A.; Liu, C. Y.; Murillo, C. A.; Villagràn D.; Wang, X. *J. Am. Chem. Soc.* **2004**, *125*, 14822. (f) D'Alessandro, D. M.; Keene, F. R.; Bergman, S. D.; Kol, M. *Dalton Trans.* **2005**, 332.

(5) (a) Plenio, H. *Organometallics* **1992**, *11*, 1856. (b) Lee, S. G.; Lee, S. S.; Chung, Y. K. *Inorg. Chim. Acta* **1999**, *286*, 215.

10.1021/om050307c CCC: $30.25
Publication on Web 08/09/2005

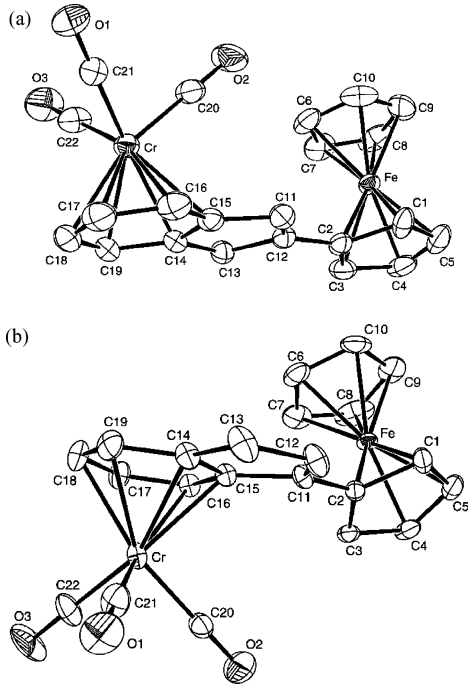

Figure 1. Molecular structures of **1** (a) and **2** (b). Hydrogen atoms have been omitted for clarity.

The molecular structures[6] of [η^6-(2-ferrocenyl)indene]-$Cr(CO)_3$ (**1**) and [η^6-(3-ferrocenyl)indene]-$Cr(CO)_3$ (**2**) are shown in Figure 1 with the atom-numbering scheme. The most relevant geometrical parameters are reported in Table 1.

The structure of complex **1** shows a *cisoid* orientation of the two metals with respect to the indene plane (Figure 1a) and reveals quite interesting features: (i) very short contact distances arise between H(6) and the O(2) C(20) carbonyl group: H(6)−O(2) (2.560(5) Å), H(6)−C(20) (3.025(6) Å); (ii) the $Cr(CO)_3$ tripod usually in the energetically stable *staggered exo* conformation assumes the uncommon *eclipsed* orientation;[7] (iii) the torsion angle C(3)−C(2)−C(12)−C(13) is here ca. 6°, which allows the plane C(1),C(2),C(3),C(4),C(5) to almost bisect the angle H(13a)−C(13)−H(13b), thus optimizing the intramolecular contact interactions of H(3) with H(13a) and H(13b), and H(1) with H(11), all in the range of 2.5−2.6 Å. The resulting Cp−indenyl is almost planar, a conformation that favors the π-electron resonance in the corresponding conjugated atom grouping of the bridging ligand. From a steric perspective, these features could be easily avoided with a *transoid* orientation of the metals.

To give an explanation of these facts, it is possible to assume that either the contact distances from H(6) to O(2) and C(20) are on the contrary stabilizing interactions of π-hydogen bond type[8] or the molecules in such *cisoid* conformation produce a better crystal packing. The hypothesis of a relatively strong bond interaction between H(6) and the carbonyl group C(20)−O(2), i.e., the presence of a typical π-hydogen bond, seems to be at least the most reasonable; this bond stabilizes and therefore justifies the observed *cisoid* conformation.

Table 1. Selected Experimental and Calculated Interatomic Distances (Å) and Torsion Angles (deg) for Complexes 1 and 2

	1[a]	**1**[b]	**1**[c]
Fe−Q(1)	1.642(1)	1.671	1.663
Fe−Q(2)	1.641(1)	1.658	1.650
Fe−Cr	6.269(2)	6.404	6.392
Cr−Q	1.744(1)	1.761	1.754
$Cr-C(O)_{av}$	1.827(6)	1.837	1.836
C(2)−C(12)	1.461(6)	1.451	1.449
C(3)−C(2)−C(12)−C(13)	−6.1(7)	−10.0	−10.2
C(1)−C(2)−C(12)−C(11)	−10.2(7)	−11.5	−12.1
H(6)−O(2)	2.560(5)	2.504	2.708
H(6)−C(20)	3.025(6)	3.155	3.244
	2[a]	**2**[b]	**2**[c]
Fe−Q1	1.653(1)	1.667	1.662
Fe−Q2	1.635(1)	1.661	1.652
Fe−Cr	5.777(2)	5.913	5.897
Cr−Q	1.747(1)	1.755	1.744
$Cr-C(O)_{av}$	1.821(6)	1.838	1.837
C(2)−C(11)	1.464(5)	1.464	1.463
C(3)−C(2)−C(11)−C(15)	−34.3(4)	−31.5	−31.7
C(1)−C(2)−C(11)−C(12)	−31.8(7)	−27.8	−27.6
H(3)−H(16)	2.380(1)	2.258	2.264

[a] Crystallographic values. [b] Nonrelativistic TZP frozen core calculations. [c] ZORA TZP all-electron calculations.

The molecular structure of complex **2** (Figure 1b) shows a disposition of the metals of *transoid* type. The tripod $Cr(CO)_3$ is in its usual more stable *staggered exo* conformation, and the torsion angle C(3)−C(2)−C(11)−C(15) is ca. 35°, as expected for optimal interactions between adjacent H atoms, all in the range of 2.4−2.7 Å. It is interesting to note that, in the presence of a less extended conjugated system, no high resonance effect and thus no planarity in the Cp-indenyl bridging ligand are to be expected here. There are no contact distances H···CO typical of π-hydrogen bonds.

IR spectra of the complexes **1** and **2** were recorded in CH_2Cl_2 at different temperatures. In the carbonyl stretching region the spectrum of isomer **1** at −80 °C showed with respect to the spectrum at 25 °C (i) a shift toward lower frequencies of the A_1 ($\Delta\nu \approx -15$ cm^{-1}) and E ($\Delta\nu \approx -20$ cm^{-1}) bands of the $Cr(CO)_3$ tripod (local symmetry C_{3v}) and (ii) the splitting of the degenerate band E ($\Delta\nu \approx 15$ cm^{-1}). In agreement with the crystallographic data the low-temperature features may be attributed to the hydrogen bonding observed in the structure in the solid state, leading to a breaking of the local symmetry. In contrast, the IR spectrum of isomer **2** showed only slight temperature dependence of the carbonyl stretching.

DFT Analysis. The crystallographic structures of the two heterobimetallic isomers **1** and **2** were optimized using DFT methods without any constraint[9] (see Supporting Information). The most relevant experimental and calculated interatomic distances and angles are reported in Table 1, using the numbering scheme of Figure 1. There is very good agreement between the

(6) Crystal data for **1**: $C_{22}H_{16}O_3CrFe$, $M = 436.20$, monoclinic, space group $P2_1/c$, $a = 12.029(3)$, $b = 10.442(2)$, $c = 15.187(3)$ Å, $\beta = 105.70(3)°$, $V = 1836.4(7)$ Å^3, $T = 293(2)$, $Z = 4$, $D_c = 1.578$ g cm^{-3}, μ(Mo Kα) = 1.401 mm^{-1}, 4324 reflections measured on a Philips PW1100 instrument. Refinement of 3929 reflections with $I \geq 2\sigma I$ converged at final R1 = 0.0609 and wR2 = 0.1455. Crystal data for **2**: $C_{22}H_{16}O_3CrFe$, $M = 436.20$, monoclinic, space group $P2_1$, $a = 11.005(3)$, $b = 7.315(2)$, $c = 11.760(3)$ Å, $\beta = 94.92(3)°$, $V = 943.2(2)$ Å^3, $T = 293(2)$, $Z = 4$, $D_c = 1.536$ g cm^{-3}, μ(Mo Kα) = 1.364 mm^{-1}, 2499 reflections measured on a Philips PW1100 instrument. Refinement of 2367 reflections with $I \geq 2\sigma I$ converged at final R1 = 0.0350 and wR2 = 0.0906.

(7) Rogers, R. D.; Atwood, J. L.; Albright, J. L.; Lee, W. A.; Rausch, M. D. *Organometallics* **1964**, *3*, 263.

(8) Stainer, T.; Tamm, M.; Lutz, B.; van der Maas, J. J. *J. Chem. Soc., Chem. Commun.* **1996**, 1127.

crystallographic experimental and computed geometries of **1** and **2**. In particular, in the optimized structure of **1** the two metal groups are disposed in a *cisoid* orientation, the torsion angle about the C(2)−C(12) bond is about 10°, and the $Cr(CO)_3$ exhibits eclipsed orientation. Instead, in the optimized structure of **2** the *transoid* arrangement of the metal groups is maintained and the bridge shows a torsion angle about the C(2)−C(12) bond of almost 30°. The carbonyls of the $Cr(CO)_3$ unit are disposed in a *staggered exo* conformation. The ZORA/TZP all-electron level of theory does not lead to significant improvements of the geometries, and this result allowed us to safely use the less expensive TZP frozen-core basis sets without including relativistic effects.

A fragment analysis was carried out at the DFT level, decomposing both the neutral complexes in the ferrocenyl-indene unit and the chromium tricarbonyl group (see Figure 2). In principle, it would be expected that the valence MOs are formed by MO interactions between the two fragments. The d(π)-MOs of the $Cr(CO)_3$ are lower in energy than those of the ferrocenyl-indene unit, and they contribute almost insignificantly to the highest occupied levels. In particular, in complex **1** the three highest occupied levels of $Cr(CO)_3$ interact with the HOMO and HOMO−2 of ferrocenyl-indene; HOMO−1, which is closely spaced to HOMO, is totally nonbonding, and back-bonding occurs through HOMO−4. In complex **2** the occupied levels HOMO and HOMO−1 are closely spaced and are localized on the ferrocenyl moiety (more than 99%), with strong metal-d character (79% and 81%). The three highest occupied MOs are nonbonding orbitals of the ferrocenyl-indene fragment. HOMO−3 is stabilized by back-bonding from the HOMO of $Cr(CO)_3$ to the LUMO of ferrocenyl-indene. In both complexes **1** and **2** the LUMOs are delocalized all over the molecular backbone with noticeable contribution of orbitals of the bridge and of the carbonyl groups, i.e., 91% and 79%, respectively. The Kohn−Sham HOMOs and LUMOs of complexes **1** and **2** are shown in Figure 3.

The different *cisoid* and *transoid* orientation of the two metal groups in the isomers **1** and **2** and the different electronic structures lead us to foresee a variation in the extent of the electronic communication in the corresponding mixed valence species $\mathbf{1}^+$ and $\mathbf{2}^+$. The localized nature of the HOMOs in both the neutral isomers suggests that the oxidation occurs at the iron and that no significant structural rearrangement takes place upon oxidation. The contribution of chromium orbitals to the HOMO of **1**, which is absent in the HOMO of **2**, is in favor of a more efficient metal−metal interaction in $\mathbf{1}^+$. Nevertheless, the cations deserve careful scrutiny since the quasi-degeneracy of HOMO and HOMO−1 present in both the neutral complexes will probably lead to a configuration interaction with the corresponding modification of the order of the energy levels.

Cyclic Voltammetry. The electrochemical oxidation by cyclic voltammetry (CV) of the bimetallic complexes **1** and **2** and, for comparison purposes, of the monometallic compounds (2-ferrocenyl)indene (**3**), (3-ferrocenyl)-indene (**4**), and η^6-$Cr(CO)_3$-indene (**5**) was obtained in CH_2Cl_2/0.1 M n-Bu_4NBF_4. The voltammetric behavior of the two complexes is quite analogous, and the CV data relative to the anodic scan at 0.5 V s^{-1} of all the quoted complexes are reported in Table 2. Scanning up to the potential of 1.1 V vs SCE, two oxidation processes occur for complexes **1** and **2**, the first one at the iron center and the second one at the chromium center. The potential peak values of the two waves, E_p, and the half-peak width, $(\Delta E_{1/2})_2 = (E_p - E_{p/2})_2$, remain almost constant even at high scan rate up to 50 V s^{-1}, as expected for monoelectronic waves when the redox process is chemically and electrochemically reversible.

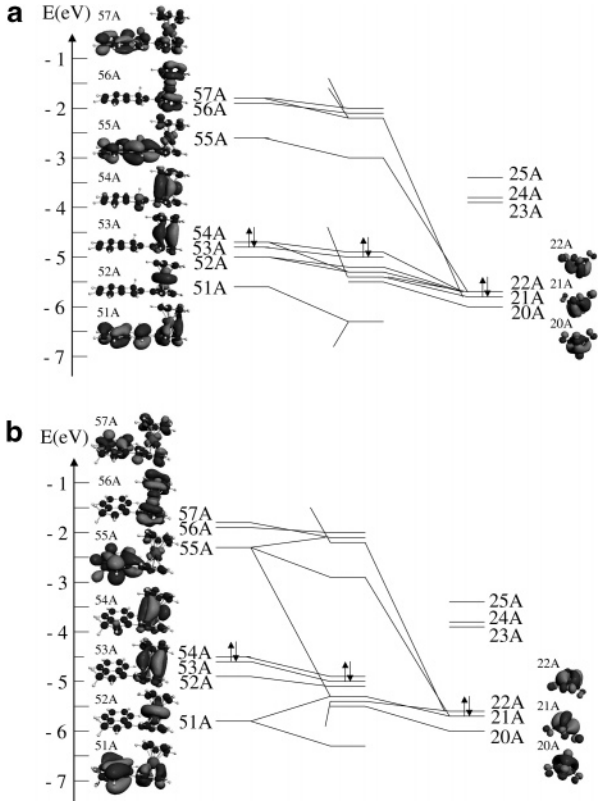

Figure 2. Interaction diagrams calculated at DFT level of theory for **1** (a) and **2** (b). Distances between almost degenerate levels are magnified. Contributions less than 5% are not shown. The occupation of the highest levels is indicated by the arrows.

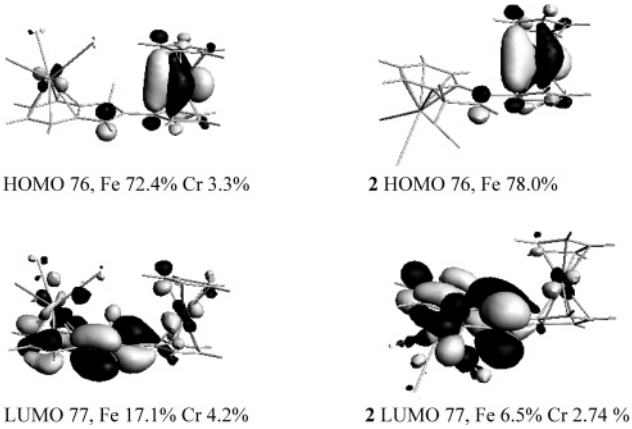

Figure 3. Kohn−Sham highest occupied molecular orbitals (HOMOs) and lowest unoccupied molecular orbitals (LUMOs) of **1** and **2** and metal percentage in their composition.

(9) (a) te Velde, G.; Bickelhaupt, F. M.; van Gisbergen, S. J. A.; Fonseca Guerra, C.; Baerends, E. J.; Snijders, J. G.; Ziegler, T. Chemistry with ADF. *J. Comput. Chem.* **2001**, *22*, 931. (b) Fonseca Guerra, C.; Snijders, J. G.; te Velde, G.; Baerends, E. J. *Theor. Chem. Acc.* **1998**, *99*, 391. (c) *ADF 2006.01*, SCM, Theoretical Chemistry, Vrije Universiteit, Amsterdam: The Netherlands, http://www.scm.com.

Table 2. Electrochemical Data[a]

complex	E_p		$E_{1/2}$		$E_p - E_{p/2}$[b]		i_a/i_c	
1	0.57	0.87	0.53	0.83	65	69	0.98	0.95
2	0.59	0.88	0.55	0.85	69	63	0.92	0.84
Fc	0.51		0.48		63		0.98	
3	0.50		0.47		67		0.97	
4	0.51		0.48		70			
5			0.77			72		0.73

[a] Solvent was CH_2Cl_2, supporting electrolyte 0.1 M *n*-Bu_4NBF_4, scan rate 0.5 V s^{-1}. All potential are in volts relative to SCE. [b] Data in mV.

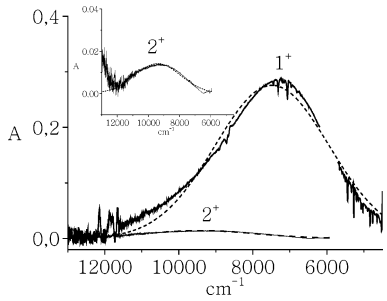

Figure 4. Near-IR spectra of 3.0 mM $\mathbf{1}^+$ and $\mathbf{2}^+$ in CH_2Cl_2 at −80 °C.

The $E_{1/2}$ values for the first oxidation process are slightly higher than those of **3** and **4**, as expected on the basis of the electron-withdrawing nature of the indene-$Cr(CO)_3$. Similarly, the second oxidation process occurs at more positive potential because of the positive charge in $\mathbf{1}^+$ and $\mathbf{2}^+$.[2h] Interestingly, the peak separation of the two waves in **1** (300 mV) and **2** (290 mV) is exactly the same as found between **5** and **3**, and **5** and **4**. On the basis of these results, it appears that the CVs of the bimetallic complexes are approximately the sum of the CVs of the monometallic compounds. However, the two isomers evidenced different behavior in the IR and near-IR spectroscopic analysis.

IR and Near-IR. The IR and near-IR measurements on $\mathbf{1}^+$ and $\mathbf{2}^+$ obtained at −80 °C by chemical oxidation with ferricinium BF_4 in CH_2Cl_2 show that electronic interaction is operating in $\mathbf{1}^+$ and much less in $\mathbf{2}^+$. In fact, in the carbonyl stretching region, the spectrum at −80 °C of the cation $\mathbf{1}^+$ showed a shift toward higher frequencies of the A_1 ($\Delta\nu \approx 13$ cm^{-1}) and E ($\Delta\nu \approx 22$ cm^{-1}) bands of the $Cr(CO)_3$ tripod with respect to the spectrum of **1**. Conversely, for $\mathbf{2}^+$ the shift of the same bands is only 5 and 10 cm^{-1}. In the near-IR region, $\mathbf{1}^+$ and $\mathbf{2}^+$ showed one band at 7300 and 9300 cm^{-1}, respectively, the former being much more intense than the latter one (Figure 4). This spectral region is often diagnostic for a charge transfer process,[1,10] and the found absorptions can be assigned to intervalence charge transfer (IVCT). Thus $\mathbf{1}^+$ and $\mathbf{2}^+$ can be well described as mixed-valence species. In fact, the bandwidth of the two bands, $\Delta\nu_{1/2} \approx 3000$ (Table 3), approximates the theoretical value[11] expected for a trapped mixed-valence (class II) asymmetric complex.[12] The much more pronounced intensity of the band is in favor of stronger electronic coupling in $\mathbf{1}^+$ than in $\mathbf{2}^+$, very likely due to the planarity of the bridging ligand and the *cisoid* conformation of the two metal units, showing that the availability of a couple of strictly correlated heterobimetallic isomers is an important requirement for the fine-tuning of intramolecular electronic communication. Nevertheless, further investigations with different techniques are needed in order to get deeper insight into the nature and extent of the metal−metal interaction.

To this aim, both experimental and theoretical studies on $\mathbf{1}^+$ and $\mathbf{2}^+$ and related derivatives are in progress in our laboratories.

Table 3. NIR Data[a]

complex	ν_c found	ν_c fitted[b]	$\Delta\nu_c$ fitted[b]	$\Delta\nu_c$ calcd[c]	E_0[d]
$\mathbf{1}^+$	7300	7480	3080	3030	1290
$\mathbf{2}^+$	9300	9050	3000	3430	1130

[a] 3.0 mM solutions in CH_2Cl_2, *T* −80 °C. All units are cm^{-1}. [b] Gaussian analysis. [c] Hush equation (refs 10, 11). [d] E_0 is evaluated as the difference between the $E_{1/2}$ for $\mathbf{5/5}^+$ (minus the substituent effect of ferrocenyl group, ca. 80 mV[2h]) and the $E_{1/2}$ for $\mathbf{1/1}^+$ and $\mathbf{2/2}^+$.

Experimental Section

[η^6-(2-Ferrocenyl)indene]-$Cr(CO)_3$ (1). To $(CH_3CN)_3Cr(CO)_3$, prepared in situ by adding to $Cr(CO)_6$ (0.400 g, 1.8 mmol) CH_3CN (20 mL), heating overnight at 130 °C, and removal of the solvent under vacuum, were added (2-ferrocenyl)indene[5] (0.300 g, 1 mmol) and THF (20 mL). After stirring and heating at 60 °C, the cool mixture was filtered and the solution was evaporated under vacuum. The residue was purified by MPLC eluting with a 20% solution of Et_2O in petroleum ether. Yield: 0.262 g (60%). Crystals suitable for X-ray analysis were grown from dichloromethane and *n*-hexane solutions at −30 °C. Anal. Calcd for $C_{22}H_{16}CrO_3Fe$: C, 52.31; H, 3.70. Found: C, 52.50; H, 3.80. The NMR and IR data are reported in the Supporting Information.

[η^6-(3-Ferrocenyl)indene]-$Cr(CO)_3$ (2). The same procedure as for **1** was followed starting from (3-ferrocenyl)indene[5] (0.300 g, 1 mmol) in THF (20 mL), and $(CH_3CN)_3Cr(CO)_3$ prepared from CH_3CN (20 mL) and $Cr(CO)_6$ (0.400 g, 1.8 mmol). After purification by MPLC **2** was recovered pure. The residue was purified by MPLC eluting with a 20% solution of Et_2O in petroleum ether. Yield 54%. Pure **2** was quantitatively recovered (232 mg) by cooling at −30 °C a *n*-pentane solution of the mixture. Crystals suitable for X-ray analysis were grown from dichloromethane and *n*-hexane solutions at −30 °C. Anal. Calcd for $C_{22}H_{16}CrO_3Fe$: C, 52.31; H, 3.70. Found: C, 52.96; H, 3.82.

Acknowledgment. This work was supported in part by Ministero dell'Istruzione, dell'Università e della Ricerca MIUR, through its PRIN, Project code 2003030870, and in part by the University of Padova through its Progetto di Ricerca di Ateneo, Project Code CPDA021354. CINECA Supercomputing Center (Italy) is acknowledged for the generous allocation of computational resources.

Supporting Information Available: CV of **1** and **2** and IR spectra for $\mathbf{1/1}^+$ and $\mathbf{2/2}^+$; *xyz* coordinates of the calculated structures; computational details; ^1H and $^{13}C\{^1H\}$ NMR data; CIF files giving crystallographic data sets for **1** and **2**. This material is available free of charge via the Internet at http://pubs.acs.org.

OM050307C

(10) (a) Creutz, C. *Prog. Inorg. Chem.* **1983**, *30*, 1. (b) Chen, P.; Meyer, T. J. *Chem. Rev.* **1998**, *98*, 1439. (c) Paul, F.; Lapinte, C. *Coord. Chem. Rev.* **1998**, *178*, 431.

(11) The theoretical values were obtained by using the Hush equation, $\Delta\nu_{1/2}$ (cm^{-1}) = $[RT \ln 2(\nu_c - E_0)]^{1/2}$, where ν_c is the frequency at the center of the peak and E_0 is the energy difference between the initial and the final states evaluated from the oxidation potentials (Table 2).

(12) (a) Hush, N. S. *Prog. Inorg. Chem.* **1967**, *8*, 391. (b) Hush, N. S. *Electrochim. Acta* **1968**, *13*, 1005. (c) Hush, N. S. *Coord. Chem. Rev.* **1985**, *64*, 135.